Published in "Swiss Journal of Geosciences 111(3): 511–522, 2018"
which should be cited to refer to this work.

The Planktonic foraminifera *Globigerinoides eoconglobatus* n. sp. in a glacial–interglacial context: IODP359 Sites U1467 and U1468

Stephanie Stainbank[1] · Silvia Spezzaferri[1] · Dick Kroon[2] · Erica S. de Leau[2] · Andres Rüggeberg[1]

Abstract
Here we define a new morphospecies of planktonic foraminifera *Globigerinoides eoconglobatus* n. sp., identified from International Ocean Discovery Program (IODP) expedition 359 samples from drift deposits of the Maldives, Inner Sea. Through biostratigraphic analysis, we infer it may be the direct ancestor of *Globigerinoides conglobatus* evolving from *Globigerinoides obliquus* in the Late Miocene (Subzone M13a). *Globigerinoides eoconglobatus* n. sp. can be distinguished from *G. conglobatus* through both its morphological traits and stable isotopic signature ($\delta^{18}O$ and $\delta^{13}C$) in pre-adult and adult specimens. The most defining characteristic being its aperture height (AH). A variance in adult stable isotopic signals shows a possible difference in life strategies, possibly related to symbionts (presence/absence or concentration) and/or depth habitat. This work also tentatively shows *G. eoconglobatus* n. sp. and *G. conglobatus* abundances are linked to glacial–interglacial stages. Its low abundances and similarities to its descendent *Globigerinoides conglobatus* has likely accounted for it being unreported, until present, in both modern and fossil studies.

Keywords Planktonic foraminifera · *Globigerinoides eoconglobatus* · Stable isotopes · Maldives · IODP

1 Introduction

Globigerinoides and *Trilobatus* are two groups of planktonic foraminifera, which include species that are among the most abundant in modern oceans (e.g., Hemleben et al. 1989). The ancestry of this group has been unclear for decades and their phylogeny remains in strong debate (e.g., Takayanagi and Saito 1962; Keller 1981; Jenkins 1985; Kennett and Srinivasan 1983; Spezzaferri 1994). The taxonomic revision of this group was undertaken by the Paleogene Planktonic Foraminiferal Working Group (PPFWG) and the Scientific Committee on Oceanic Research/International Geosphere-Biosphere Programme (SCOR/IGBP) Working Group 138 "Planktonic foraminifera and ocean changes". In this framework, Spezzaferri et al. (2015) and Spezzaferri et al. (2017, in press) have clarified the phylogenetic relationship, at the beginning of the range of this group of foraminifera, based on genetic and morphological evidence. They have divided *Globigerinoides* sensu strictu from *Trilobatus*. These authors have established clear criteria to separate the two genera. Both genera are characterized by a trochospiral test and one to multiple supplementary apertures on the spiral side. However, following the classification of Hemleben and Olsson (2006), *Trilobatus* possesses a *sacculifer*-type wall texture and *Globigerinoides* possesses a *ruber*/*sacculifer* or *ruber*-type wall texture. In the now commonly accepted phylogeny, *Trilobatus* is paraphyletic and gives rise to the *Praeorbulina*/*Orbulina* and *Sphaeroidinellopsis*/*Sphaeroidinella* lineages. *Globigerinoides* can presently be considered as monophyletic and includes the species from the *Globigerinoides ruber* lineage and its descendants including *Globigerinoides conglobatus*.

Presently the Neogene Planktonic Foraminifera Working Group (NPFWG), as continuation of the PPFWG, is

Electronic supplementary material

✉ Stephanie Stainbank
stephanie.hayman@unifr.ch

[1] Department of Geosciences, Université of Fribourg, Chemin du Musée 6, 1700 Fribourg, Switzerland

[2] School of GeoSciences, Grant Institute, University of Edinburgh, The King's Buildings, James Hutton Road, Edinburgh EH9 3FE, UK

investigating planktonic foraminifera from Miocene to Present, which also includes the taxonomic revision of younger *Globigerinoides* and *Trilobatus*. As part of this effort, we present here evidence of the evolution of *Globigerinoides obliquus* into the new morphospecies *Globigerinoides eoconglobatus* n. sp., which is the ancestor of *G. conglobatus*. The occurrence of *G. eoconglobatus* n. sp. and *G. conglobatus* are also tentatively related to glacial–interglacial stages.

2 Systematic palaeontology

Order Foraminiferida d'Orbigny 1826
Superfamily Globigerinoidea Carpenter, Parker And Jones 1862
Family Globigerinidae Carpenter, Parker and Jones 1862
Genus *Globigerinoides* Cushman 1927, amended by Spezzaferri et al. 2015
Globigerinoides eoconglobatus n. sp. Stainbank, Spezzaferri, Kroon, de Leau and Rüggeberg
(Figs. 1 and 2)

Etymology Named *eoconglobatus* as in 'early or dawn' as it is the ancestor of *G. conglobatus* (Fig. 2)

Type of wall Normal perforate, cancellate, spinose, *ruber/sacculifer*-type wall texture and *conglobatus*-type wall texture of Hemleben et al. (2017, in press). The primary wall texture of *G. eoconglobatus* n. sp. is *ruber/sacculifer*-type. However, similarly to *G. conglobatus*, individuals were found with calcitic crusts with a *conglobatus*-type wall texture (Hemleben et al. 2017, in press) (Fig. 2, 5–6). This texture represents a modification of the external *ruber/sacculifer*-type wall texture: the high density of thin spines supported by short spine collars are partly covered by calcite crusts during gametogenesis. The result is a hummocky texture of overgrown spine collars, which occasionally show spine holes that may further develop in a thick euhedral calcite crust (Hemleben et al. 2017, in press).

Test morphology Low to moderately high trochospiral consisting of two whorls, quadrangular to circular in outline and markedly lobate. Chambers are subspherical, four in the last whorl gradually increasing in size. The last chamber is slightly laterally compressed. Sutures depressed and straight on both sides. Umbilicus open and deep. Primary aperture umbilical to slightly extraumbilical, medium-sized to high and a wide arch. Several small to moderately high and rounded sutural supplementary apertures on the spiral side. It has a high density of thin spines.

Size This morphospecies is generally larger than 250 μm. Maximum diameter of the holotype is 548 μm.

Distinguishing features It is distinguished from *G. obliquus* by its last chamber, which is less laterally compressed. It also has numerous supplementary apertures. It differs from *G. conglobatus* primarily by its wide, high aperture and inflated final chamber in adult specimens. An additional distinguishing feature is the coiling, which is tight and streptospiral in *G. conglobatus* and loosely coiled in *G. eoconglobatus* n. sp.

Discussion To identify *G. conglobatus* we have strictly followed the "morphospecies" concept used in Wade et al. (2017, in press). We have defined it by a series of morphological characters that are shared with the holotype. Consequently, *G. eoconglobatus* n. sp., having different characters has been identified as a new morphospecies. Therefore, both *G. conglobatus* and *G. eoconglobatus* n. sp. may or may not represent true biological species. Forms similar to *G. eoconglobatus* n. sp. have been identified as *G. conglobatus* or its synonyms by several authors (e.g., Bé and Tolderlund 1971; Fordham 1979; Rillo 2016; Rillo et al. 2016). Yet, due to the lack of accompanying figures in the majority of publications, it is difficult to ascertain the true extent of this morphospecies distribution. Currently, based on this study and images from Rillo (2016) we can state it is found in the Indian and Pacific Oceans.

Phylogenetic relationship Aze et al. (2011) reported the evolution of *G. conglobatus* from *G. obliquus* in the Late Miocene. As such, it is inferred that *G. eoconglobatus* n. sp. evolved from *G. obliquus* in Subzone M13a and gives origin to *G. conglobatus* in Zone PL1.

Stratigraphic range From Subzone M13a to Holocene.

Type Level Maldives, Inner Sea. The holotype is from drift deposits of International Ocean Discovery Program (IODP) 359 Hole U1467B, Sample 359, U1467B, 3H-3, 69–71. Recovered at 4°51.0255′N, 073°17.0204′E at 487.49 m water depth.

Geographic distribution This morphospecies is present in the Indian Ocean Sites drilled during IODP expedition 359. Rillo (2016) also reports it in the Indian and Pacific Oceans, yet it is identified as *G. conglobatus*. Further studies are, therefore, needed to confirm its presence at other locations, as the true geographical extent of this species is presently unresolved.

Stable isotope paleobiology Surface mixed layer (tropical/subtropical).

Repository Holotype (MHNF32906) and Paratypes (MHNF32907, MHNF32908, MHNF32909) are deposited in the Natural History Museum of Fribourg (NHMF), Switzerland.

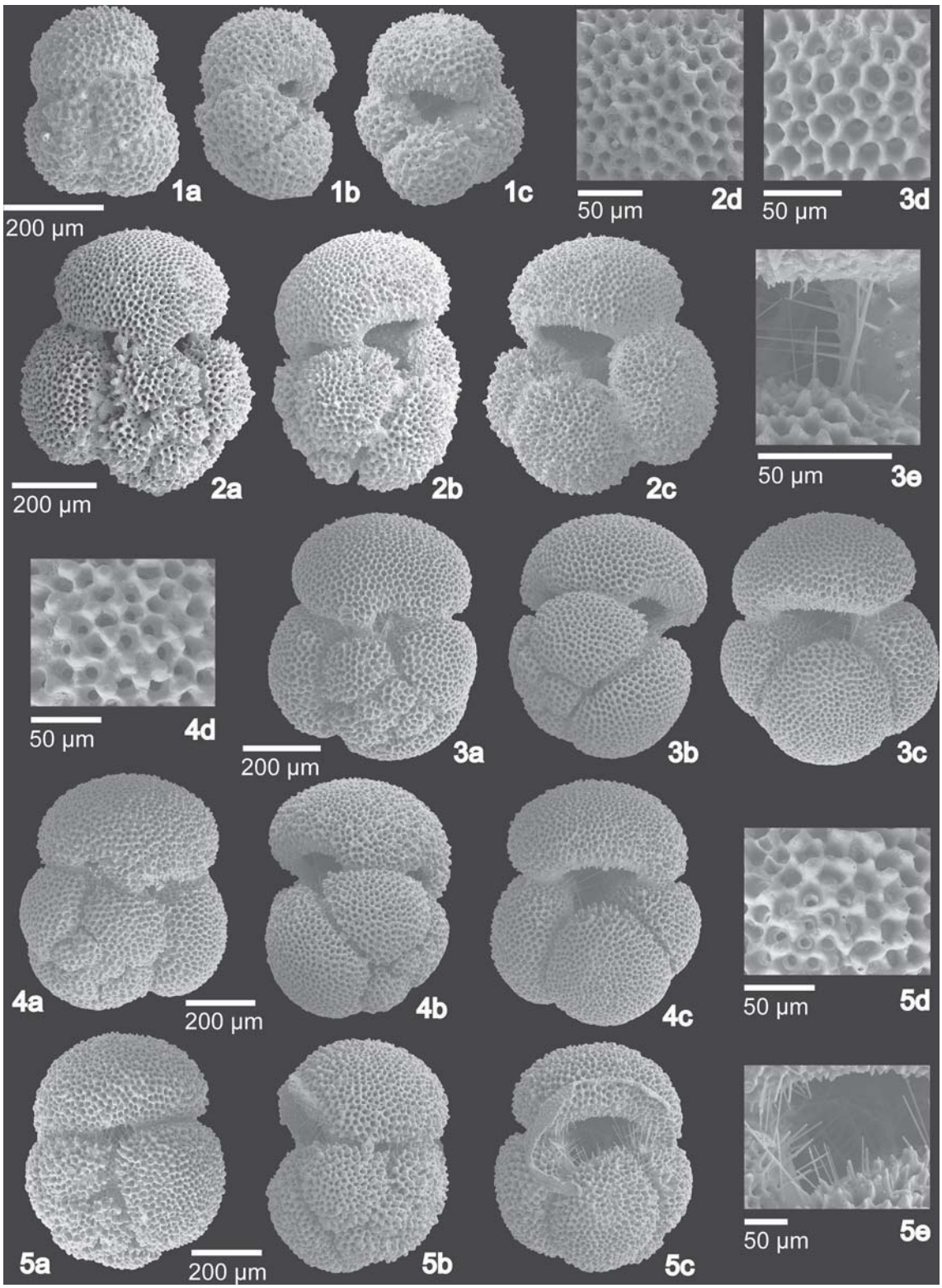

Fig. 1 Plate illustrating *Globigerinoides eoconglobatus* n. sp. Stainbank, Spezzaferri, Kroon, de Leau and Rüggeberg. **1a–c** *Globigerinoides eoconglobatus* n. sp. juvenile, Sample: 359, U1467B, 3H-3, 45–46; **2** Holotype MHNF32906, from Sample 359, U1467B, 3H-3, 69–71, **2a** spiral view, **2b** ventral view, **2c** umbilical view, **2d** wall texture, **3** Paratype MHNF32907 from Sample 359, U1468A, 1HCC, 15–20, **3a** spiral view, **3b** ventral view, **3c** umbilical view, **3d** wall texture, **3e** magnified spines; **4** Paratype MHNF32908 from Sample 359, U1468A, 1HCC, 15–20, **4a** spiral view, **4b** ventral view, **4c** umbilical view, **4d** wall texture; **5** Paratype MHNF32909 from Sample 359, U1468A, 1HCC, 15–20, **5a** spiral view, **5b** ventral view, **5c** umbilical view, **5d** wall texture, **5e** magnified spines

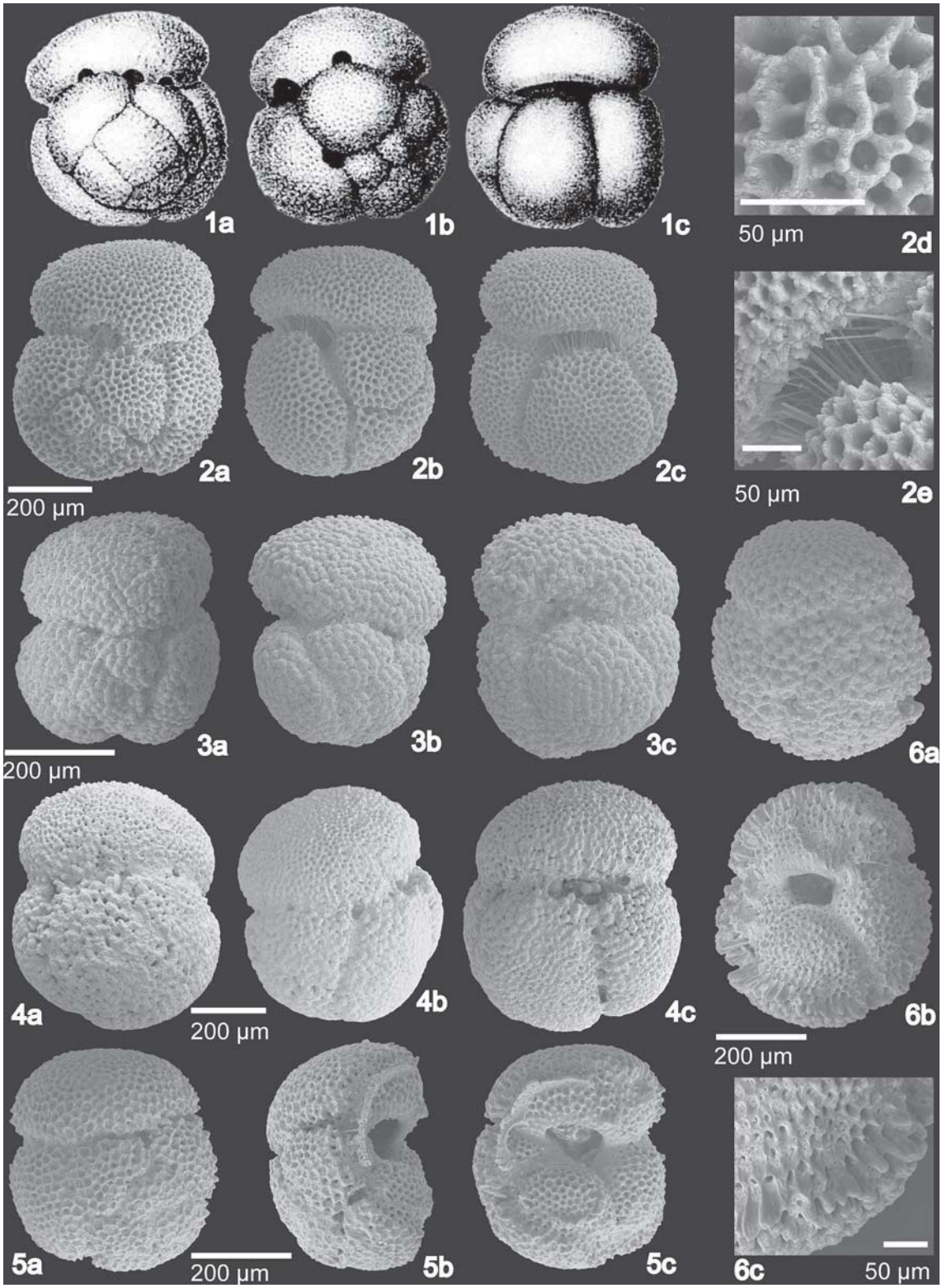

Fig. 2 Plate illustrating *Globigerinoides conglobatus* Brady 1879 and *Globigerinoides eoconglobatus* n. sp. STAINBANK, SPEZZAFERRI, KROON, DE LEAU AND RÜGGEBERG. **1a–c** (x50) *Globigerina conglobata*; **2a–e** *Globigerinoides conglobatus* from Sample 359, U1468A, 1HCC, 15–20; **3a–c** *Globigerinoides conglobatus* from Bahamas sample 1007B, 25X-2, 60–61; **4a–c** *Globigerinoides conglobatus* from Sample 359, U1467B, 3H-3, 69–71; **5a–c** and **6a–c** *Globigerinoides eoconglobatus* n. sp. with cortex from Sample 359, U1467B, 3H-3, 99–100

3 Materials and methods

All samples are from sediment cores from the IODP expedition 359, Sites U1467 (4°51.0274′N, 73°17.0223′E) and U1468 (4°55.98′N, 73°4.28′E) (Fig. 3a, b) (Betzler et al. 2016). These Sites were drilled in the Inner Sea, a drift deposit, of the Maldives Archipelago at water depths of 487 and 521.5 mbsl, respectively. The Maldives is located within the Indian Ocean off the coast of India.

Bulk samples were weighed and soaked in water for at least 12 h. Subsequently they were washed through a 32 μm sieve and dried at room temperature. Samples for quantitative analysis were reweighed after drying.

3.1 Biostratigraphy

Sets of 219 and 26 samples from Holes U1467B and U1467C respectively, were used for detailed stratigraphic assessments. This included all core catcher samples, excluding one (41F) and 142 section samples for Hole U1467B, and 14 core catcher samples supplemented by 12 section samples for Hole U1467C. Hole U1467B presented a record from the Middle/Late Miocene (Zone M10–11) to the Pleistocene (Subzone Pt1b) whereas U1467C extended from the Middle to Late Miocene (Zone M9–M12). In all samples, the entire foraminifera assemblage was documented to define the range of the new morphospecies and infer its phylogenetic relationships.

3.2 Morphometry and quantitative/qualitative assessments

Morphometric analyses were performed on 50 adult specimens each of *G. conglobatus* and *G. eoconglobatus* n. sp. Individuals were collected, from both Holocene and Pleistocene aged samples, from the > 250 μm fraction with the largest specimen being 888.08 μm in size.

Specimens were mounted in apertural view on Scanning Election Microscope (SEM) stubs using carbon glue paper and viewed under a Nikon SMZ18 stereomicroscope fitted with a 0.5× SHR Plan Apo objective. Images were taken of each specimen using the NIS Elements Imaging Software v4.60. Four parameters were measured: aperture width (AW), aperture height (AH), maximum width of specimen (W) and maximum height of specimen (H). Both AW and AH; as well as W and H were measured perpendicular to each other (Fig. 4a, b). The primary aperture diameter ratio (PADR) (Spezzaferri et al. 2015) is defined as the ratio AW/AH whereas the relative symmetry (RS) of the specimen is the ratio W/H. The multivariate statistical test, Principal Component Analysis (PCA) was performed on the morphometric data using PRIMER v6 (Clarke and Gorley 2006).

Quantitative assessments were made across Marine Isotope Stages (MIS) 11 and 12. The dust age model of U1467 of Kunkelová et al. (2018, submitted) was used to define the time points and select the appropriate samples. In total, 24 samples were sieved into the > 250 μm fraction and weighed. This procedure was used to assess absolute abundances of the two target species (*G. eoconglobatus* n. sp. and *G. conglobatus*) over a glacial–interglacial interval. Samples were split randomly into aliquots containing at least 300 specimens and the number of *G. conglobatus* and *G. eoconglobatus* n. sp. noted. Counts were standardised to 1 g for dry bulk weight.

The assessment was further extended to include an additional 29 samples for relative abundance determination. For each of the unweighed samples, counts of the two target species were noted for aliquots of 300 specimens and the relative abundances calculated.

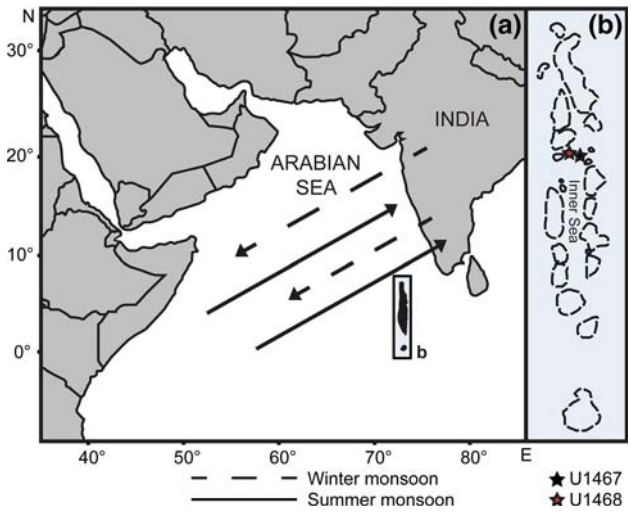

Fig. 3 **a** Location map of the study site showing the position of IODP359 Sites U1467 and U1468, **b** within the Inner Sea of the Maldives

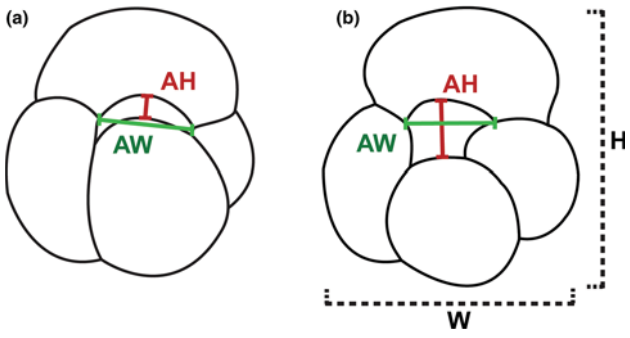

Fig. 4 Morphometric parameters measured: aperture height (AH), aperture width (AW), height of specimen (H) and width of specimen (W) for both (**a**) *G. conglobatus* and (**b**) *G. eoconglobatus* n. sp.

3.3 Multi-species stable isotopes

Stable isotopes ($\delta^{18}O$ and $\delta^{13}C$) were measured on five species (planktonic: *Globigerinoides ruber* (white), *Globigerina siphonifera, G. conglobatus*, *G. eoconglobatus* n. sp. and benthic: *Cibicides mabahethi*) to infer the preferred depth habitats (Table 1). Specimens were selected from three samples from the minimum values of MIS11. Optimal size fractions were selected individually for each species, in order to reduce isotopic offsets related to size (Birch et al. 2013; Ezard et al. 2015). Two size fractions for *G. conglobatus* and *G. eoconglobatus* n. sp. were used, 355–400 μm and 400–500 μm, as there is no consensus in the literature for an optimal size and thus pre-adult and adult specimens were analysed. Samples (~ 0.05 mg) were analyzed at The Grant Institute of the University of Edinburgh on a Thermo Electron Delta+ Advantage mass spectrometer integrated with a Kiel carbonate III automated extraction line. The instrument has an analytical precision of 0.1‰ for $\delta^{18}O$ and $\delta^{13}C$. Measurements were calibrated against the laboratories internal standard and are expressed in the standard delta notation as parts per mil (‰). Due to the small specimen number required for *G. conglobatus* and *G. eoconglobatus* n. sp. replicates were run for each sample and the mean used in the subsequent analysis.

4 Results and discussion

Globigerinoides conglobatus is a sub-tropical, spinose and symbiont-bearing species (Schiebel and Hemleben 2017). It hosts dinoflagellates and inhabits the deeper photic zone of the surface mixed layer (Ezard et al. 2015; Schiebel and Hemleben 2017). Overall, *G. conglobatus* has a low abundance (0.1–4.9%) in the world's tropical and subtropical ocean surface waters (e.g., Bé and Tolderlund 1971; Ovechkina et al. 2010; Rippert et al. 2016). Kroon (1988) reported relative abundances for the > 250 μm fraction in the summer surface waters (0–5 m) ranging from ~ 18% in the North-Eastern Indian Ocean to ~ 9% in the Arabian Sea. Bé and Tolderlund (1971) noted its highest abundances in North Pacific and North Atlantic surface waters with maximum relative abundances of up to 74% reported during October and November in the central North Atlantic.

Table 1 Isotope parameters used for each species

Species	Size fraction (μm)	No. specimens analysed
G. ruber$_w$	212–250	5
G. siphonifera	300–355	2
G. conglobatus /	355–400	2
G. eoconglobatus n. sp.	400–500	1
C. mabahethi	> 250	3

Globigerinoides conglobatus has a wide distribution and is extensively referenced in the literature. However, considering the distinct similarities between *G. conglobatus* and *G. eoconglobatus* n. sp. it is likely that the latter has been identified as *G. conglobatus* in a number of past studies. This is certainly the case in the Henry Buckley Collection (Rillo 2016; Rillo et al. 2016), with images, of numerous specimens collected from plankton tows and sediment samples in the Indian and Pacific Oceans, recorded as *G. conglobatus* which can now be identified as *G. eoconglobatus* n.sp. Yet, as the majority of authors do not include plates or figures it is difficult to discern the extent of these inconsistencies or the inferred geographical range of *G. eoconglobatus* n. sp. Furthermore, recognised synonymies of *G. conglobatus* could also contribute to these uncertainties, as in the case of Fordham (1979) whereby Plate 10, Fig. 12 (pg. 318) bears a resemblance to *G. eoconglobatus* n. sp. but has been called *Globigerinoides canimarensis,* a species now placed in synonymy with *G. conglobatus* (Young et al. 2017).

4.1 Biostratigraphy

Following identification of all species present in the samples, planktonic foraminifera (PF) Zones were identified using the classifications of Wade et al. (2011). Not all marker species were present and thus not all Zones or Subzones could be conclusively defined. Consequently, a number of Zones were grouped together. Holes U1467B and U1467C encompassed Zones PT1b—M10 and M12—M9, respectively (Fig. 5).

Aze et al. (2011) reports the appearance of *G. conglobatus* in the Late Miocene, shortly after *Globigerinoides extremus*, with both having *Globigerinoides obliquus* as a common ancestor. Our data contributes to these inferred phylogenetic relationships with the addition of *G. eoconglobatus* n. sp. in the stratigraphic range. In our samples, *G. eoconglobatus* n. sp. appears shortly after *G. extremus* within the Subzone M13a. However, *G. conglobatus* only first occurs in Zone PL1, ~ 4 Myr later. Subsequently, we propose that *G. eoconglobatus* n. sp. evolved from *G. obliquus* and from which the typical form of *G. conglobatus* evolved in the Early Pliocene. With both *G. conglobatus* and *G. eoconglobatus* n. sp. having a shared ancestor, *G.obliquus*, the similarities in morphology are apparent. *Globigerinoides conglobatus* is an extant species and *G. eoconglobatus* n. sp. is present, based on Rillo (2016), (e.g. catalogue numbers: PM ZF 7058, PM ZF 7060 and PM ZF 7068), in the modern Indian Ocean at least up until 50 years ago. Thus further studies are needed to clarify its presence in modern oceans.

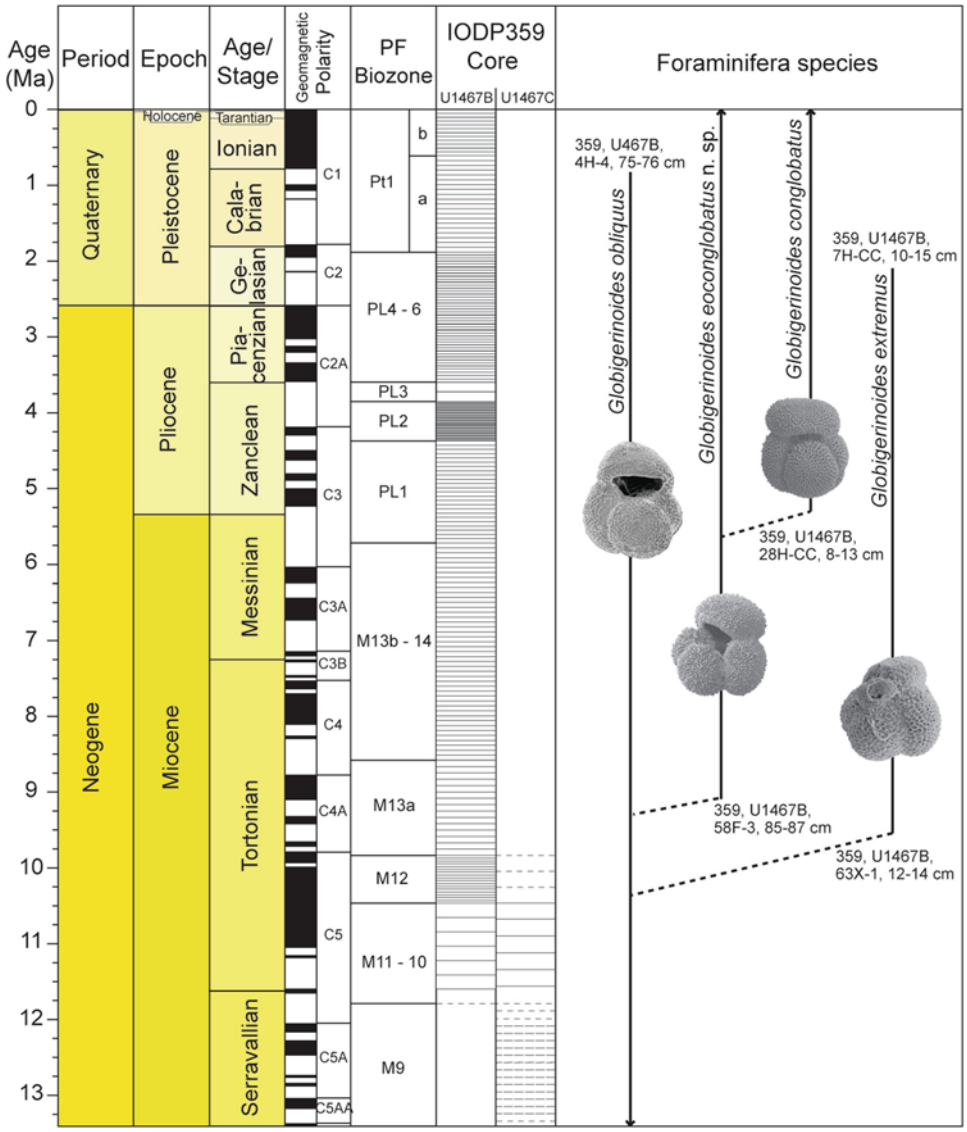

Fig. 5 Stratigraphic range and inferred phylogenetic relationships of *G. eoconglobatus* n. sp. from IODP359 Site U1467. Note planktonic foraminifera Zones are adapted from Wade et al. (2011) and reflect those that were identifiable within our samples. Dashed lines within the IODP359 cores reflect sample boundaries whereby the exact start or end point is uncertain. Dashed lines for the foraminiferal species show surmised phylogenetic relationships. Holotype image of *G. obliquus* is from Spezzaferri and Olsson (2017, in press). All other images are taken from the IODP359 samples, with *G. extremus* representing the first occurrence

4.2 Morphometry and quantitative/qualitative assessments

The PADR, AW/AH, ranged from 2.93 to 6.42 with an average of 3.99 ± 0.71 for *G. conglobatus* (Fig. 6a). On the contrary, the *G. eoconglobatus* n. sp. PADR ranged from 1.31 to 2.68 with an average of 1.91 ± 0.30. The ∼ 2× higher PADR observed for *G. conglobatus* can be accounted for by the larger AH of *G. eoconglobatus* n. sp. *G. conglobatus* AW were ∼ 4 times greater than the AH, whereas *G. eoconglobatus* n.sp. aperture was more symmetrical. Overall, both species are similarly symmetrical showing near-spherical tests with RS averages of 0.93 ± 0.04 and 0.89 ± 0.04, respectively (Fig. 6b). As seen in Fig. 6a, c, PADR clearly separates the two datasets with no distinguishable separation observable across the RS parameter (Fig. 6b, c).

A statistically strong linear correlation (R^2 = 0.7299) is observed between AW and AH for *G. conglobatus* (Fig. 6d) yet this trend is not observed for *G. eoconglobatus* n. sp. (R^2 = 0.5173). This shows that the evolution of the aperture width and height, through the growth stages (pre-adult to adult) of *G. conglobatus* is near symmetrical in its size advances. On the contrary, the *G. eoconglobatus* n. sp. morphometric data shows the AH increases significantly in size over its lifespan, yet the AW does not mimic this expanse. The large, open aperture was the initial difference noted between these two species and thus our data reinforces this feature as an important identifiable criterion for the new morphospecies.

A Principal Component Analysis (PCA) distinguished two principal components that explained 97% of the data variance (PC1: 92.7% and PC2: 4.3%) (Fig. 7). PC1 was negatively correlated with both specimen width (W:

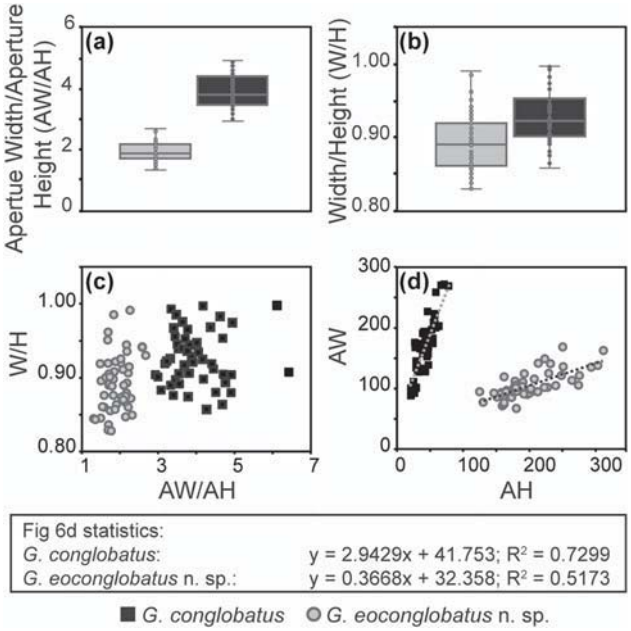

Fig. 6 **a** Box plots showing the comparison of the primary aperture diameter ratio (PADR: AW/AH) and **b** the relative symmetry (RS: W/H) for both *G. conglobatus* (black) and *G. eoconglobatus* n. sp. (grey), **c** and **d** scatter plots showing the relationship between measured morphometric parameters W, H, AW and AH

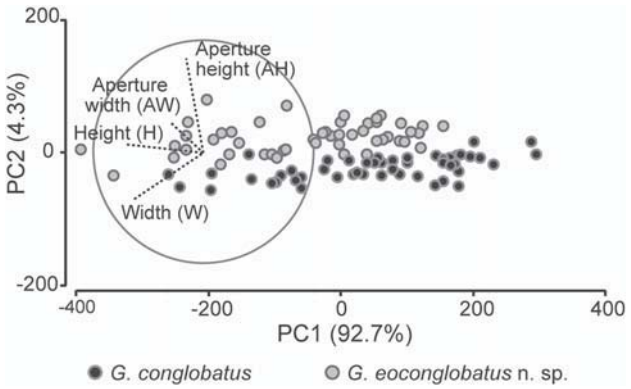

Fig. 7 Principal Component Analysis (PCA) derived from the morphometric data of *G. conglobatus* (black circles) and *G. eoconglobatus* n. sp. (grey circles). The Spearman rank correlation vectors of the morphometric variables are plotted (dashed lines)

$\lambda = -0.633$) and specimen height (H: $\lambda = -0.699$). Aperture height was positively correlated with PC2 (AH: $\lambda = -0.861$). PC1 represents the size distribution of the sample set, which included pre-adults and adults, thus this variable was anticipated to be discriminating within our dataset. Therefore, AH is the most discriminating parameter measured, with the two sample sets separated out across the entire H range (407.83–888.08 μm). This shows the metric is consistent as a defining feature within adult specimens and further supports the data obtained from the morphometric analysis.

Globigerinoides conglobatus and *G. eoconglobatus* n. sp. both have low relative abundances in the Maldivian MIS11–12 samples (Fig. 8). Contributions ranged from 0–2.0% for *G. conglobatus* and 0–3.65% for *G. eoconglobatus* n. sp with absolute abundances ranging from 0–52 and 0–107 ind/g, respectively.

Quantitative counts, standardised to dry bulk weight (g) showed two distinct trends between the *G. conglobatus* and *G. eoconglobatus* n. sp. datasets (Fig. 8). The absolute abundances of the former remain relatively consistent between glacials–interglacials, fluctuating around 21 ind/g. On the contrary, a distinct disparity can be seen during MIS11 with a marked increase in *G. eoconglobatus* n. sp. during the interglacial. In the majority of the samples, *G. eoconglobatus* n. sp. concentrations are constantly higher (mean: 39 ind/g) than *G. conglobatus* (mean: 21 ind/g), and increase two/three fold directly after the glacial maxima. *Globigerinoides eoconglobatus* n. sp. showed an increase during the start of deglaciation and peaks just before the MIS11 minima before showing a gradual trend back to comparative *G. conglobatus* values. The relative abundances reflect the same trend, and show a constant fluctuation around the means towards the glacial maximum of MIS10. However, as abundances are low, further sampling needs to be carried out in order to evaluate the significance of these trends.

Interesting to note, in a 2003 summer monsoon June/July sampling campaign in the Arabian Sea, Seers et al. (2012) reported no *G. conglobatus* in their foraminifera assemblage data. Whether this was due to the lack of specimens or an extremely low abundance is unclear. However, this highlights the variability of the species, having been reported in low (9–18%), but substantial abundances in a summer Arabian Sea study by Kroon (1988). Clearly, *G. conglobatus* thrives during certain seasons and/or oceanographic conditions with both Bé and Tolderlund (1971) and Kennish (2000) recognising *G. conglobatus* as an autumn species. Already present in low abundances, this could have accounted for the morphospecies being overlooked in this region until present.

4.3 Stable isotopes

Stable isotopic compositions of planktonic foraminifera tests yield extensive information relating to environmental conditions (including but not limited to temperature, ice volumes and ambient seawater compositions) and their preferred living depths (e.g., Ezard et al. 2015). Samples from MIS11 were chosen because this long interglacial warm period is generally recognised as a potential analog for the Holocene. Subsequently, MIS11 can provide an ideal framework to identify the preferred habitat of the new morphospecies within the context of our five target species.

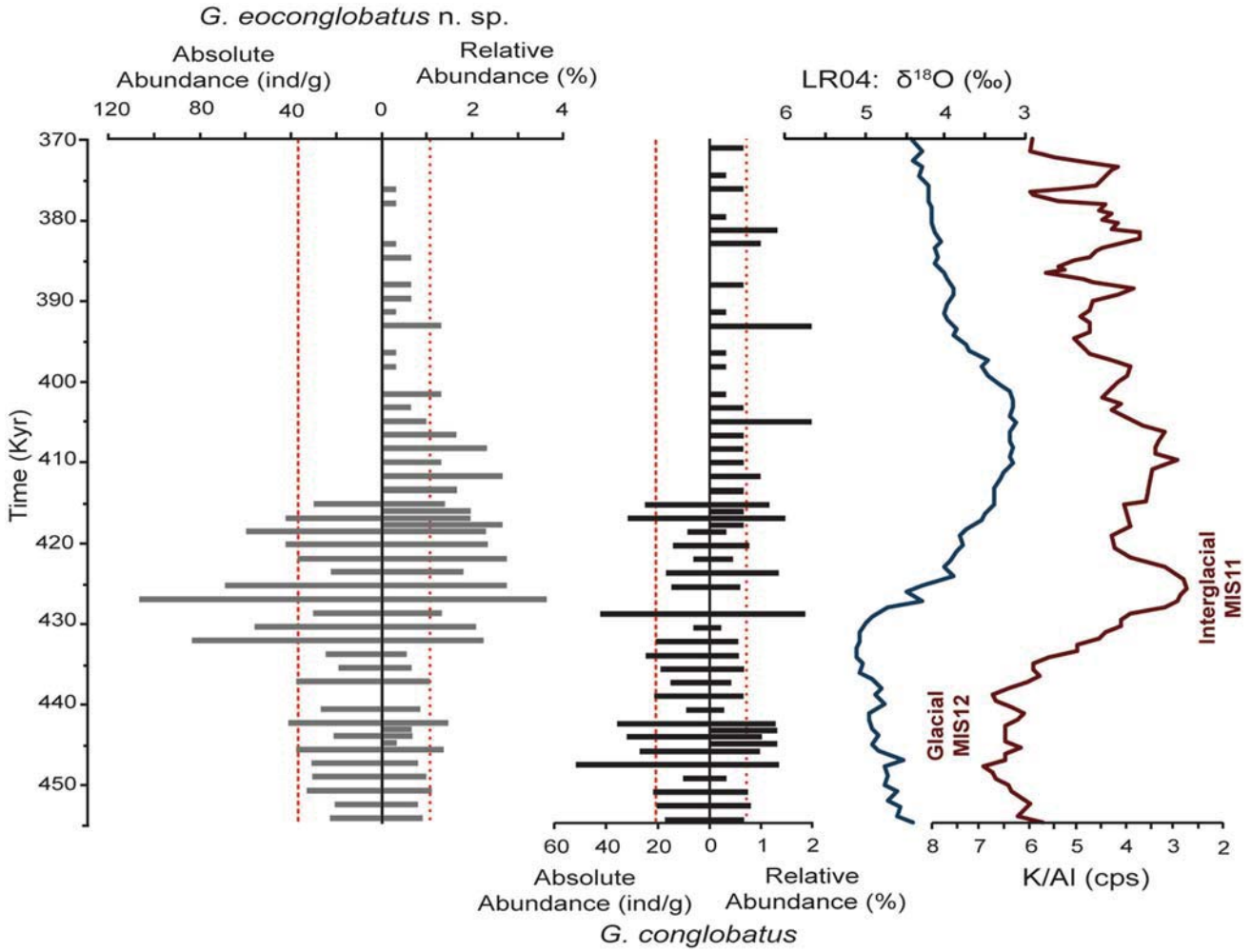

Fig. 8 Abundance data for *G. conglobatus* and G. *eoconglobatus* n. sp. together with the K/Al age model from IODP359 Site U1467 (Kunkelová et al. submitted) and global ice volume benthic foraminifera LR04 stack (Lisiecki and Raymo, 2005). Dashed red lines indicate mean abundances

The $\delta^{18}O$ values ranged from − 1.80 to − 1.05‰ for *G. conglobatus* and − 2.06 to − 1.34‰ for *G. eoconglobatus* n. sp. (Online Resource 1). Similarly, the $\delta^{13}C$ values ranged from 1.21 to 2.03 and 0.79 to 1.66‰ for the two species. An outlier was identified from the larger *G. conglobatus* size fraction and removed from the dataset. For the larger size fraction, as only one specimen was analysed, it is plausible that some form of contamination from taphonomic processes could have occurred. Therefore, to avoid any discrepancies in the analysis, it was excluded.

A size related effect is evident between the species in both isotopic signals ($\delta^{18}O$ and $\delta^{13}C$) with a distinct separation for the larger fraction (400–500 μm) (Fig. 9a). As such, an overlap in the isotopic values appears to be limited to the smaller size fraction (300–355 μm). Both the $\delta^{18}O$ and $\delta^{13}C$ values display the same disparity from pre-adult to adult stage with *G. conglobatus* recording a heavier- and *G. eoconglobatus* n. sp. a lighter signal shift. Even though their respective depth habitats, surmised from the $\delta^{18}O$ values, change between pre-adult and adults both morphospecies are constrained between *G. ruber* and *G. siphonifera* (Fig. 9b). Thus, both appear to occupy the surface mixed layer.

Figure 9c shows the comparison of the position of the IODP359 isotopic signals from the Indian Ocean in relation to the isotopic signals of *G. conglobatus* of the same size fractions from the Atlantic (Williams et al. 1981; Ravelo and Fairbanks 1992, 1995; Keigwin et al. 2005) and Pacific Oceans (Berger et al. 1978). Regardless of the small sample size and scattered data points, the same shift from low to high values is recorded within the $\delta^{18}O$ signals. No data was available for the larger size fraction in the Pacific Ocean and thus the single data point, from the smaller fraction, was included merely for comparison of the preferred depth habitat.

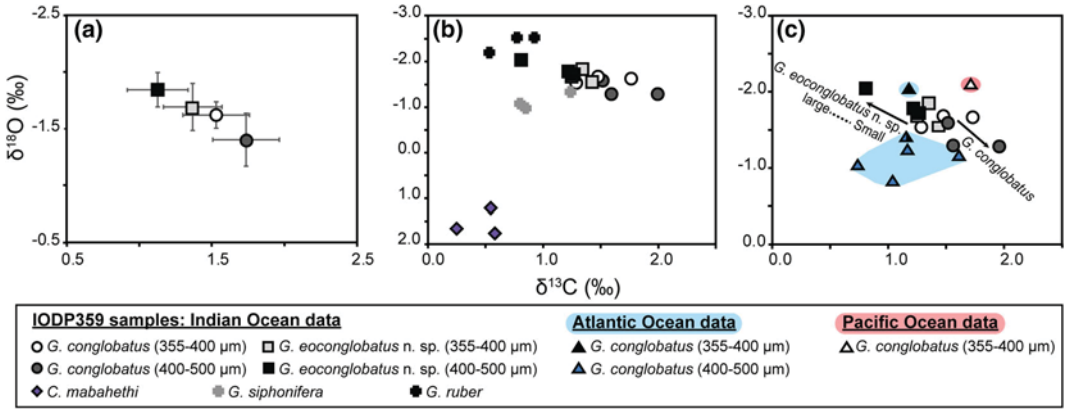

Fig. 9 Stable isotope ($\delta^{18}O$ and $\delta^{13}C$) values of *G. eoconglobatus* n. sp. and *G. conglobatus* from the IODP359 samples in the Indian Ocean (**a, b, c**) including reference taxa (**b, c**) *G. conglobatus* from the Pacific (Berger et al. 1978) and Atlantic (Williams et al. 1981; Ravelo and Fairbanks 1992, 1995, Keigwin et al. 2005) Oceans

Several working hypotheses could explain these differences in the isotopic signals as being related to i) different gametogenic processes and/or ii) symbionts. Adult *G. conglobatus* migrate to sub-surface waters and produce a gametogenetic calcite crust (Hemleben et al. 2017, in press). This strategy is evident in our samples with a higher $\delta^{18}O$ signal for the 400–500 µm fraction. Additionally, these encrusted individuals encompass the vast majority of the *G. conglobatus* specimens in dead assemblages. On the contrary, *G. eoconglobatus* n. sp. adults appear to prefer shallower waters. Yet interesting to note are Fig. 2, 5–6 displaying *G. eoconglobatus* n.sp. individuals with an apparent thick calcitic crust. It is difficult to accurately disentangle the actual mechanisms surrounding this calcite crust development as currently they are not entirely constrained, and no intact individuals bearing this crust were found, for *G. eoconglobatus* n. sp. According to Ezard et al. (2015) different ocean basins, presence as well as the type of symbionts are the primary controls in size-dependent $\delta^{13}C$ and $\delta^{18}O$ shifts. Spero (1998) has noted that *G. conglobatus* exhibited a large intraspecific range for both $\delta^{13}C$ and $\delta^{18}O$ within studies and, therefore, it cannot be excluded that these trends could represent natural variation within each species.

5 Conclusions

The distinction of new species must always be made with caution, in order to avoid confusion within the taxonomy. Extensive taxonomic revisions are ongoing (e.g. PPFWG, NPFWG), in order to recognise and disentangle synonymies and consolidate the existing foraminifera taxa. In this regard, here we contribute to this effort and define *G. eoconglobatus* n. sp. as a new morphospecies, based on a combination of morphological, biostratigraphic, stable isotope and abundance data. *Globigerinoides eoconglobatus* n. sp. may or may not represent a true biological species but it is a distinguishable geological morphospecies with significance in biostratigraphy. *Globigerinoides eoconglobatus* n. sp. was identified from International Ocean Discovery Program (IODP) expedition 359 samples from drift deposit sediments of the Maldives, Inner Sea. Based on biostratigraphical assessments, it is inferred that it is the direct ancestor of *G. conglobatus* and evolved from *G. obliquus* in the Late Miocene.

Morphological differences to *G. conglobatus*, was the initial criterion noted for our new morphospecies. Subsequently, various statistical tests, identified aperture height (AH) as the most distinguishing feature within pre-adults and adults. Besides distinctive morphological differences, discrete shifts in abundances in relation to glacial–interglacial intervals was also apparent. *Globigerinoides eoconglobatus* n. sp. showed a marked increase during the interglacial/post-interglacial. On the contrary, *G. conglobatus* abundances remained relatively constant during the glacial–interglacial interval. Interpretation of the stable isotopic signals is complicated (Ezard et al. 2015). Yet, from our preliminary data *G. eoconglobatus* n. sp. shows an inverse isotopic trend (higher to lower) in comparison to *G. conglobatus* (lower to higher). Whether these differences are related to symbionts, life strategies or natural variation within the populations is uncertain at the current stage of our research.

Acknowledgements The authors would like to thank the International Ocean Discovery Program for supplying the samples used in our study. Colin Chilcott is acknowledged for assistance during the stable isotope analysis at the Grant Institute, University of Edinburgh. The two anonymous reviewers are thanked for their valuable comments on the manuscript. This study was supported by funding from the Swiss National Science Foundation (200021_165852/1).

References

Aze, T., Ezard, T. H. G., Purvis, A., Coxall, H. K., Stewart, D. R. M., Wade, B. S., et al. (2011). A phylogeny of Cenozoic macroperforate planktonic foraminifera from fossil data. *Biological Reviews, 86,* 900–927.

Bé, A. W. H., & Tolderlund, D. S. (1971). Distribution and ecology of living planktonic foraminifera in surface waters of the Atlantic and Indian Oceans. In B. M. Funnell & W. K. Riedel (Eds.), *Micropaleontology of marine bottom sediments* (pp. 105–149). Cambridge: Cambridge University Press.

Berger, W. H., Killingley, J. S., & Vincent, E. (1978). Stable isotopes in deep-sea carbonates: Box Core ERDC-92, West Equatorial Pacific. *Oceanologica Acta, 1*(2), 203–216.

Betzler, C. G., Eberli, G. P., Alvarez Zarikian, C. A., & The Expedition 359 Scientists. (2016). Expedition 359 preliminary report: Maldives monsoon and sea level. *International Ocean Discovery Program.* https://doi.org/10.14379/iodp.pr.359.2016.

Birch, H. S., Coxall, H. K., Pearson, P. N., Kroon, D., & O'Regan, M. (2013). Planktonic foraminifera stable isotopes and water column structure: Disentangling ecological signals. *Marine Micropaleontology, 101,* 127–145.

Clarke, K. R., & Gorley, R. N. (2006). *Primer v6: User manual/tutorial*. Plymouth: PRIMER-E.

Ezard, T. H. G., Edgar, K. M., & Hull, P. M. (2015). Environmental and biological controls on size-specific $\delta^{13}C$ and $\delta^{18}O$ in recent planktonic foraminifera. *Paleoceanography, 30,* 151–173.

Fordham, B.G. (1979). A chronocladogeny and corresponding classification of Neogene planktic foraminifera with a documentation of morphotypes from two Pacific deepsea stratigraphic sections. *Ph.D. dissertation*, University of Queensland, Australia.

Hemleben, C., & Olsson, R. (2006). Wall textures of Eocene planktonic foraminifera. In P.N. Pearson, R.K. Olsson, B.T. Huber, C. Hemleben & W.A. Berggren (Eds.), *Atlas of Eocene Planktonic Foraminifera*, pp. 47–66), Cushman Foundation for Foraminiferal Research, Special Publication No. 41.

Hemleben, C., Olsson, R.K., Premac-Fucek, V., Hernitz-Kucenjac, M. (2017). Wall textures of Oligocene normal perforate planktonic Foraminifera, pp. 55–78). In *Cushman Foundation Special Publication No. 46, Chapter 3* **(in press)**.

Hemleben, C. H., Spindler, M., & Anderson, O. R. (1989). *Modern planktonic foraminifera (363 pp)*. New York: Springer.

Jenkins, D. G. (1985). Southern mid-latitude Paleocene to Holocene planktic foraminifera. In H. M. Bolli, J. B. Saunders, & K. Perch-Nielsen (Eds.), *Plankton stratigraphy* (pp. 263–288). Cambridge: Cambridge Earths Science Series, Cambridge University Press.

Keigwin, L. D., Bice, D. M., & Copley, N. J. (2005). (Table 2) Stable isotopes of planktonic foraminifera in MOCNESS samples off Cape Cod. *PANGAEA*. https://doi.org/10.1594/pangaea.835234.

Keller, G. (1981). Origin and evolution of the genus *Globigerinoides* in the Early Miocene of the northwestern Pacific, DSDP Site 292. *Micropaleontology, 6,* 269–295.

Kennett, J. P., & Srinivasan, M. S. (1983). *Neogene Planktonic Foraminifera, a phylogenetic Atlas*. Stroudsburg: Hutchinson Ross Publishing Co.

Kennish, M. J. (2000). *Practical handbook of marine science* (3rd ed.). Boca Raton: CRC Press.

Kroon, D. (1988). Distribution of extant planktic foraminiferal assemblages in Red Sea and Northern Indian Ocean surface waters. In G.-J. A. Brummer & D. Kroon (Eds.), *Planktonic Foraminifers as tracers of ocean-climate history* (pp. 229–267). Amsterdam: Free university Press.

Kunkelová, T., Jung, J.A., de Leau, E.S., Odling, N., Thomas, A.L., Betzler, C., Eberli, G.P., Alvarez-Zarikian, C.A., Alonso-Garcia, M., Bialik, O.M., Blättler, C.L., Guo, J.A., Haffen, S., Horozal, S., Hui Mee, A.L., Inoue, M., Jovane, L., Lanci, L., Laya, J.C., Lüdmann, T., Nath, B.N., Nakakuni, M., Niino, K., Petruny, L.M., Pratiwi S.D., Reijmer, J.J.G., Reolid, J., Slagle, A.L., Sloss, C.R., Su, X., Swart, P.K., Wright, J.D., Yao, Z., Young, J.R., Lindhorst, S., Hayman-Stainbank, S., Rüggeberg, A., Spezzaferri, S., Carrasqueira, I., Yu, S., Kroon, D. (2018). A two million year record of continental weathering linked to aridity from the Maldives. Progress in Earth and Planetary Science **(submitted)**.

Lisiecki, L. E., & Raymo, M. E. (2005). A Pliocene-Pleistocene stack of 57 globally distributed benthic $\delta^{18}O$ records. *Paleoceanography*. https://doi.org/10.1029/2004pa001071.

Ovechkina, M. N., Bylinskaya, M. E., & Uken, R. (2010). Planktonic foraminiferal assemblage in surface sediments from the Thukela Shelf, South Africa. *African Invertebrates, 51,* 231–254.

Ravelo, A. C., & Fairbanks, R. G. (1992). Oxygen isotopic composition of multiple species of planktonic foraminifera: Recorders of the modern photic zone temperature gradient. *Paleoceanography, 7*(6), 815–831.

Ravelo, A. C., & Fairbanks, R. G. (1995). Carbon isotopic fractionation in multiple species of planktonic foraminifera from core-tops in the tropical Atlantic. *Journal of Foraminiferal Research, 25*(1), 53–74.

Rillo, M.C. (2016). Dataset: Henry Buckley collection of planktonic foraminifera. *Natural History Museum Data Portal* (data.nhm.ac.uk). https://doi.org/10.5519/0035055

Rillo, M.C., Whittaker, J., Ezard, T.H.G., Purvis, A., Henderson, A.S., Stukins, S., Miller, C.G. (2016). The unknown planktonic foraminiferal pioneer Henry A. Buckley and his collection at The Natural History Museum, London. *Journal of Micropalaeontology*, *36*, 191–194. https://doi.org/10.1144/jmpaleo2016-020

Rippert, N., Nürnberg, D., Raddatz, J., Maier, E., Hathorne, E. C., Bijma, J., et al. (2016). Abundance of planktic foraminifera measured on multinet samples at station SO225_21. *PANGAEA*. https://doi.org/10.1594/pangaea.864438.

Schiebel, R., & Hemleben, C. (2017). *Planktic foraminifers in the Modern Ocean*. Berlin: Springer.

Seers, H.A., Darling, K.F., Wade, C.M. (2012). Ecological partitioning and diversity in tropical planktonic foraminifera. *BMC Evolutionary Biology*, 12(54) 1–15.

Spero, H. (1998). Life history and stable isotope geochemistry of planktonic foraminifera. *The Paleontological Society Papers, 4,* 7–36.

Spezzaferri, S. (1994). Planktonic foraminiferal biostratigraphy and taxonomy of the Oligocene and lower Miocene in the oceanic record. An overview. *Paleontographia Italica*, *81*, 187.

Spezzaferri, S., Kucera, M., Pearson, P. N., Wade, B. S., Rappo, S., Poole, C. R., et al. (2015). Fossil and genetic evidence for the polyphyletic origin of the planktonic foraminiferal genus *Globigerinoides* and the description of the new genus *Trilobatus*. *PLoS One, 10*(5), e0128108. https://doi.org/10.1371/journal.pone.0128108.

Spezzaferri, S., Olsson, R.K., Hemleben C. (2017, in press). Taxonomy, biostratigraphy, and phylogeny of Oligocene to Lower Miocene Globigerinoides and Trilobatus, pp. 269–306. In Cushman Foundation Special Publication No. 46, Chapter 9.

Takayanagi, Y., & Saito, T. (1962). Planktonic foramnifera from the Nobori Formation, Shikoku, Japan. *Science Reports, N5,* 67–106. **(Tohoku University, Special)**.

Wade, B. S., Pearson, P. N., Berggren, W. A., & Pälike, H. (2011). Review and revision of Cenozoic tropical planktonic foraminiferal biostratigraphy and calibration to the geomagnetic

polarity and astronomical time scale. *Earth-Science Reviews, 104,* 111–142.

Wade, B.S, Pearson, P.N., Olsson, R.K., Silva, I.P., Berggren, W.A., Spezzaferri, S, Huber, B. T., Coxall, H.K., Fucek, V.P., Kucenjak. M.H., Hemleben, C., Leckie, M.R., Smart, C.W. (2017, in press). Taxonomy, biostratigraphy, phylogeny and diversity of Oligocene and Early Miocene planktonic foraminifera, pp. 11–28. In *Cushman Foundation Special Publication No. 46,* Chapter 1.

Williams, D. F., Be, A. W. H., & Fairbanks, R. G. (1981). Seasonal stable isotopic variations in living planktonic foraminifera from Bermuda plankton tows. *Palaeogeography, Palaeoclimatology, Palaeoecology, 33*(1–3), 71–102.

Young, J.R., Wade, B.S., Huber, B.T. (Eds.) pforams@mikrotax website. 6 November 2017. http://ww.mikrotax.org/pforams.